Diffusion of Dextran in Aqueous (Hydroxypropyl)cellulose

Z. Bu and P. S. Russo*

Department of Chemistry and Macromolecular Studies Group, Louisiana State University, Baton Rouge, Louisiana 70803-1804

Received August 9, 1993; Revised Manuscript Received November 15, 1993®

ABSTRACT: Fluorescence photobleaching recovery (FPR) was used to measure the probe self-diffusion coefficients, D_s, of eight labeled dextrans with different molecular weights in aqueous solutions of the semirigid polymer (hydroxypropyl)cellulose (HPC). With added measurements of free dye and a single dye-labeled polymeric latex, the probe hydrodynamic radius, R_h, spanned 5–551 Å. For dextrans, the dependence of D_s upon M obeys $D_s \sim M^{-\beta}$ with $\beta \approx {}^1/_2$ in water. In the most concentrated HPC solution studied, $\beta \approx 1$. Small probes show strong deviations from the Stokes–Einstein relation. The effect was less severe as probe size increased. Most of the diffusion data fit the Langevin–Rondelez equation, $D_s/D_0 = \eta_0/\eta + \exp[-(R_h/\xi)^\delta]$, where D_0 and η_0 are respectively the diffusion coefficient in and viscosity of pure solvent, ξ is the correlation length, and δ a parameter. Exceptions to the Langevin–Rondelez relation were found for small probes in dilute solution ($R_h/\xi < 0.1$). The data are also interpreted using the hydrodynamic scaling model advanced by Phillies and a cylindrical cell model developed by Johansson and co-workers. The effect of the molecular weight of the HPC matrix upon the diffusion of variously sized probes was also studied; small probes were relatively insensitive to matrix molecular weight, but the diffusion of larger probes did depend on the molecular weight of the HPC. Analytical applications of FPR are considered. HPC selectively retards dextrans according to molecular weight, the effect becoming stronger as HPC concentration is increased. The FPR signal for a mixture of two dextrans with different molecular weights can be markedly biexponential in HPC solution, even if it is not pure water. This expansion of the recovery time distribution by the polymer matrix suggests that FPR in a polymer matrix can serve as a medium-resolution method to detect macromolecular polydispersity, similar in spirit to analytical gel electrophoresis but applicable to uncharged polymers, suitably labeled. A preliminary evaluation is promising.

Introduction

Translational mobility of polymers in complex solutions is relevant to basic aspects of macromolecular science ranging from viscosity of coatings to rates of intracellular biotransport. Measurements of the diffusion of a probe particle through a polymeric matrix have proven illuminating,[1-27] although the area could hardly be called mature. In a paper closely related to the present study, Furukawa et al.[15] provide a succinct and penetrating account of the difficult problems that remain; recent reviews provide more detail.[3,16] The present study addresses one particular question, the transition from "small probe" to "large probe" behavior. The mesoscopic probes to be discussed are larger than solvent molecules but smaller than typical latex particles. They also possess a more complex structure.

The various types of systems that have been studied can be distinguished by the nomenclature probe/matrix/solvent. An extensively studied class is hard sphere/linear polymer/solvent.[1-14] If the hard spheres, usually latex particles or colloidal silica, scatter strongly compared to the matrix, dynamic light scattering may be used. In aqueous systems, it is not usually possible to match the matrix index of refraction to that of the solvent. Background scattering is inevitable and experiments must be carried out with large probes that scatter very strongly compared to the matrix. Systems involving less massive probes, such as linear coils or star polymers,[17-27] require very careful refractive index matching that is only possible in organic solvents. Even if the refractive index matching is perfect, there is some controversy regarding how dynamic light scattering experiments from ternary solutions should be interpreted.[28] In comparison, optical tracer techniques, such as forced Rayleigh scattering[29] or fluorescence photobleaching recovery (FPR),[30,31] provide unambiguous probe diffusion coefficients over a very wide range.

(Hydroxypropyl)cellulose (HPC) has been used as a matrix material in several studies.[5-11,50] This propyl-substituted, β-1,4-linked polysaccharide is relatively stiff (persistence length ~100 Å[32-34]). High, non-Newtonian viscosities are achieved at low concentrations where matrix scattering and matrix-probe compatibility problems are small. At very high concentrations (avoided in the present study) HPC has a lyotropic mesophase.[35,36] HPC is uncharged, so the electrostatic contributions to the dynamics are just those due to the dilute probe particles. The disadvantages of HPC are also noteworthy. Even after fractionation, it is not monodisperse. This problem is ameliorated by the availability of a wide range of molecular weights, which permit at least a qualitative study of the effect of matrix molecular weight. The stiffness of HPC is high compared to most polymers, but structures of far greater rigidity do exist—e.g., synthetic polypeptides, DNA, certain mineral fibers, and wholly aromatic backbone polymers. HPC is effectively a copolymer, since the degree of propyl ether substitution on any monomeric repeat unit varies. Finally, HPC is slightly hydrophobic; its stability in water depends on a hydration shell that vanishes at temperatures exceeding ~ 40 °C, depending on the degree of propyl substitution.[11,37]

Previous studies in HPC[5-11] suggested that mesoscopic probe behavior would be observed for probes with radii of approximately 10–1000 Å. Dextrans conveniently span much of this range. Dextrans are also polysaccharides, but their predominant α-1,6-linkages are more flexible than the β-1,4-links in HPC; the persistence length of dextran is probably less than 20 Å.[38,39] Dextran appears to be less hydrophobic than HPC. A limited number of 1,3-linkages cause dextran to be slightly branched. The nature of the branching is controversial; some groups report short branches grafted to the main chain,[39] while others argue in favor of longer, randomly placed branches.[40] In

* To whom correspondence should be addressed.
® Abstract published in *Advance ACS Abstracts*, January 15, 1994.

0024-9297/94/2227-1187$04.50/0

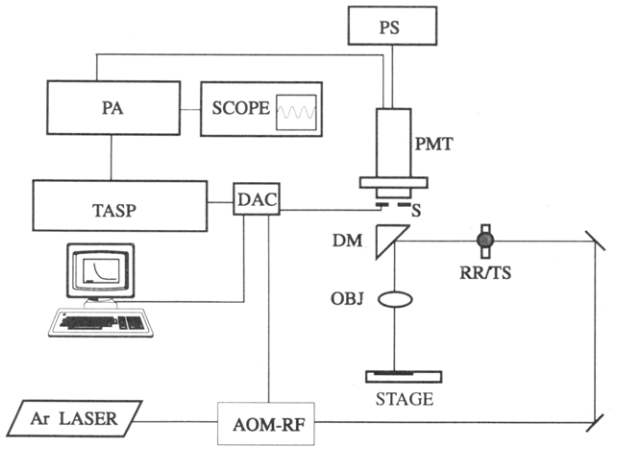

Figure 1. Schematic of FPR instrument. AOM = acoustooptic modulator; RF = radio-frequency driver for AOM; RR = Ronchi ruling; TS = transverse slide; DM = dichroic mirror; S = shutter; PS = power supply; PMT = photomultiplier tube; PA = preamplifier; TASP = tuned amplifier/synchronization/peak voltage detection circuits; DAC = data acquisition and control interface.

the context of the present study, it suffices to point out that dextran is not a hard-sphere probe particle.

Experimental Procedure

HPC samples of nominal molecular weights 60 000, 300 000, and 1 000 000 were purchased from Scientific Polymer Products, Inc. The catalog numbers were 402, 403, and 404, respectively. The polymers were used as received. HPC was dissolved in water containing 3 mM NaN_3 to prevent bacterial growth. Dissolution of HPC in water took 2 weeks or longer, depending on the molecular weights and concentrations. Solutions were prepared to known weight fractions w_{HPC}, and the conversion to concentration c used previously determined partial specific volume data.[11] Diffusion coefficients of fluorescein (as the disodium salt) in water and HPC solutions were obtained from previous studies.[11]

Eight dextran fractions labeled with fluorescein isothiocyanate (FITC–dextran) were purchased from Sigma. The claimed molecular weights were 3900 (Lot No. 57F-0016), 9000 (Lot No. 67F-5031), 18 900 (Lot No. 45F-0275), 40 500 (Lot No. 125F-0124), 71 600 (97F-0599), 148 900 (126F-0144), 506 000 (Lot. No. 27F-5064), and 2 000 000 (Lot No. 27F-5045). Aliquots from fresh stock solutions of FITC-labeled dextrans were added to the HPC solutions; the final dextran probe concentration was always less than 14 μg/mL.

Fluorescent latex of advertised diameter 0.13 μm was purchased from Polysciences Inc. (Fluoresbrite plain microspheres, 1% solids). The latex solution was diluted 60-fold prior to measuring the diffusion coefficient in water. The latex probe content in the HPC solutions was about 0.004%. Mixing of the latex with HPC solutions caused aggregation, which could be observed in the FPR epifluorescence microscope. This process was reversed by adding a small amount (about 0.1%) of the surfactant, Triton-X100. Samples were stirred, loaded into 0.2-mm-path-length microslide cells (Vitro dynamics Inc.), and flame sealed for FPR measurement. The fluorescent intensity was weak compared to that of FITC–dextran/HPC solutions, but signal quality was still adequate.

Viscosities were measured on a Bohlin CS cone and plate rheometer at 30 ± 0.5 °C. The shear rates were 2–40 Hz for 0.453% and 1.07% HPC solutions and 0.04–0.600 Hz for 2.422% and 3.871% solutions. Shear thinning effects were negligible under these conditions.

The FPR instrument (Figure 1) is built around an Olympus BH2 epifluorescence microscope, using FITC filter cubes. Most of the illuminator assembly is removed to permit rear illumination by a Lexel Model 3000 argon ion laser producing up to 1.8 W at 488 nm. The laser beam is passed through a Newport Research 35085 acoustooptic modulator (AOM) driven by a modified 31085-6DS radio-frequency source from the same manufacturer. Measurement and bleaching are both performed with the first-order diffracted beam; the contrast between on (bleaching) and off (reading) states for this beam is selectable between 10000:1 and 2000:1 and the latter value was always used. About 85% of the laser output can be switched into the first-order diffraction spot with negligible alteration of position or the Gaussian beam profile. A coarse diffraction grating, or Ronchi ruling (Edmund Scientific), is mounted on a transverse slide assembly and brought into the rear focal plane of the microscope objective. Available diffraction gratings are 50, 100, 150, 200, and 300 lines/in.; available microscope objectives are 4×, 7×, 10×, and 18×. The grating constant, $K = 2\pi/L$, where L is the period of the repeat pattern in the sample, is determined by microphotometry for any particular combination of Ronchi ruling and microscope objective. The transverse slide upon which the Ronchi rulings are mounted is designed to effect modulation detection, as first described by Lanni and Ware.[30,31] The key part is a bidirectional worm gear/pawl assembly taken from a bait-casting fishing reel (Penn Peerless No. 9, Wal-Mart). A low-voltage dc motor drives the worm gear; the Ronchi rulings are attached to the pawl assembly. An appropriate prebleach dc signal level is established by adjusting the high-voltage gain of the photomultiplier tube and the gain/filtering stages of the Stanford Research Systems SR560 preamplifier. Next, the motor is stopped and the shutter (Newport 846HP) is closed to protect the RCA 7265 photomultiplier tube (PMT) from overexposure during the photobleaching pulse. The AOM is turned on for a predetermined time (ideally and almost always in this study $<0.1\Gamma^{-1}$, where Γ is the recovery rate) to create the transient grating in the sample. When the AOM is turned off, shutter reopened, and motor restarted, the movable and permanent illumination grating falls into and out of coincidence with the stationary but transient sample grating to produce a weak triangle ac oscillation superimposed upon a strong dc signal. As the pattern fades, the triangle wave becomes more rounded and the ac voltage swing diminishes exponentially at a rate proportional to the diffusion coefficient. The fundamental frequency of the oscillating signal must match one of several settings (16, 32, 48, or 96 Hz) of a custom-built tuned circuit that isolates and amplifies the ac component. The system is tuned prior to an actual experiment and usually optimized each time a new Ronchi ruling is inserted. Therefore, the most convenient way to change the spatial frequency K is by altering objectives, not Ronchi rulings. Tuning is accomplished by bleaching a permanent pattern in FITC-labeled gelatin[41,42] and adjusting motor speed to maximize the output of the tuned amplifier circuit. An oscilloscope or spectrum analyzer is helpful during tuning, but not necessary. The output of the tuned amplifier closely approximates a sine wave. Its amplitude is determined by a peak voltage detection (PVD) circuit.[43] The PVD is reset each time the ac signal crosses ground from below and stores the maximum value for any given cycle one-fourth of a cycle later. A trigger signal is produced on crossing ground in the opposite direction; it is logically "anded" with a signal derived from a photocell that determines when the Ronchi ruling is at full speed (i.e., sufficiently far from a turnaround point). When the trigger signal and photocell reading are both "true", the dc and ac voltages are read, time is determined to ±0.05 s, and all three values are written to the fixed disk of an IBM PC-AT computer equipped with an IBM data acquisition and control adapter. The decay of the ac signal is typically observed for a time window equal to $10/\Gamma$. To prevent enormous data files, some measurement cycles may be skipped during slow recoveries. The data are read back from disk and smoothed to produce recovery profiles containing approximately 100 points. Under these measurement conditions, the ac voltage obeys a simple decay law:[30,31] ac volts = $\exp(-\Gamma t)$ with $\Gamma = DK^2$ where D is the diffusion coefficient and t the time since photobleach. The ac signal may be ratioed to dc to account for parasitic photobleaching during the recovery time, drift in laser intensity, AOM characteristics, or motor speed; however, this was not necessary for the present experiments. The decay rates were extracted by a nonlinear least-squares Marquardt algorithm to one (or more) exponentials plus a floating base line, after assigning the uncertainties by an interactive graphical process. Diffusion coefficients were obtained as the slopes of Γ vs K^2 plots; typically, 2–5 repeat measurements were made at each of 3–4 K values.

Table 1. Diffusion Coefficients of Dextrans in HPC and Other Parameters (See Text)

w_M	0	0.004 53	0.010 70	0.024 22	0.038 71
c_M[a]/g·mL^{-1}	0	0.004 51	0.010 67	0.024 22	0.038 83
η/cP	0.8904	6.277	24.4	628	4670
	$D_s/10^{-7}$ cm^2 s^{-1} at 25 °C				
fluorescein[b] (R = 5.02 Å, M = 332, α = 15 ± 4,[c] ν = 1.1 ± 0.4[c])	48.8	47.8	44.0	31.7	29.2
FD-4 57F-0016 (R_h = 13.2 Å, M_w = 3900, M_w/M_n < 1.5, α = 19 ± 9,[c] ν = 1.3 ± 0.8[c])	21.0 ± 0.4	17.4 ± 0.5	21.5 ± 1	13.0 ± 0.4	11.3 ± 0.3
FD-10 67F-5031 (R_h = 16.9 Å, M_w = 9000, α = 13 ± 2,[c] ν = 0.9 ± 0.15[c])	15.4 ± 0.2	13.7 ± 0.3	13.3 ± 0.7	10.9 ± 0.3	8.68 ± 0.4
FD-20 45F-0275 (R_h = 27.8 Å, M_w = 18 900, α = 24 ± 1,[c] ν = 0.71 ± 0.02[c])	9.96 ± 0.1	8.0 ± 0.3	6.9 ± 0.3	5.1 ± 0.1	3.77 ± 0.06
FD-40 125F-0124 (R_h = 44.5 Å, M_w = 40 500, α = 35 ± 1,[c] ν = 0.71 ± 0.01[c])	6.2 ± 0.2	4.79 ± 0.02	3.8 ± 0.1	2.5 ± 0.1	1.84 ± 0.04
FD-70 97F-0599 (R_h = 57.8 Å, M_w = 71 600, α = 54 ± 2,[c] ν = 0.67 ± 0.03[c])	4.8 ± 0.1	3.20 ± 0.01	2.48 ± 0.06	1.40 ± 0.01	0.92 ± 0.03
FD-150 126F-0144 (R_h = 88.0 Å, M_w = 148 900, M_w/M_n < 1.35, α = 67 ± 1,[c] ν = 0.78 ± 0.02[c])	3.15 ± 0.06	2.14 ± 0.02	1.45 ± 0.04	0.72 ± 0.01	0.415 ± 0.01
F-7638 27F-5046 (R_h = 133 Å, M_w = 506 000, α = 106 ± 11,[c] ν = 0.87 ± 0.14[c])	2.09 ± 0.03	1.30 ± 0.01	0.588 ± 0.01	0.247 ± 0.006	0.144 ± 0.01
FD-2000S 27F-5045 (R_H = 179 Å, M_w = 2 000 000, α = 170 ± 3,[c] ν = 0.84 ± 0.02[c])	1.55 ± 0.03	0.70 ± 0.01	0.291 ± 0.005	0.064 ± 0.01	
latex (R_h = 551 Å, M_w = 4 × 10^6, α = 311 ± 2,[c] ν = 0.83 ± 0.01[c])	0.503 ± 0.007	0.134 ± 0.009	0.0339 ± 0.001	0.0018 ± 0.0001	
$\xi_{LR,linearized}$[c]/Å		200	90	50	30
$\delta_{LR,linearized}$		0.44	0.81	0.82	0.69
$\xi_{LR,nonlinear}$/Å		189 ± 34	90 ± 6	46 ± 6	28 ± 3
$\delta_{LR,nonlinear}$		0.46 ± 0.06	0.82 ± 0.07	0.64 ± 0.09	0.56 ± 0.07
ξ_c/Å		480	360	273	234
$\xi_{HS,nonlinear}$/Å		333 ± 42	103 ± 11	46 ± 6	25 ± 3
$\delta_{HS,nonlinear}$		0.63 ± 0.05	0.96 ± 0.12	0.64 ± 0.08	0.56 ± 0.07

[a] Computed from the weight fraction using partial specific volume measured at 30 °C for water and HPC, respectively: v_1 = 1.0047 mL/g and v_2 = 0.8057 mL/g.[11,67] [b] D_s for fluorescein (disodium salt) measured at 25 °C, corrected to T = 30 °C.[11] Error ≈ ±5%. [c] Computed from unweighted nonlinear least-squares fit to eq 2 using g/mL for the unit of concentration. [d] Concerning the uncertainty in this parameter, see the text.

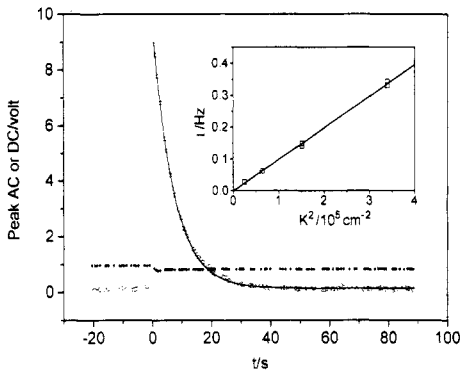

Figure 2. Recovery profile for FD-10 in 2.422% HPC (300 K) solution; K = 389 cm^{-1}. The solid curve is a single-exponential fit with a floating base line. Inset: Γ vs K^2 for the same sample.

The precision is ±2% in concentrated solutions and ±12% for dilute or weakly fluorescent samples. All diffusion measurements were made at 30.0 ± 0.2 °C.

Probe Diffusion Results and Discussion

A typical recovery profile appears in Figure 2. The inset shows a plot of Γ vs K^2; the zero intercept, within uncertainty, implies the absence of convection and/or chemical recovery of the dye. All the diffusion data are summarized in Table 1, along with other system parameters and some of the scaling results to be discussed below.

Scaling Analysis. Three symbols signifying molecular weight are used during the discussion: M_p, the molecular weight of the probe; M_m, the matrix molecular weight; and sometimes M, the polymer molecular weight when discussing theoretical predictions for binary solutions. The dependence of diffusion upon M_p is shown in Figure 3. In

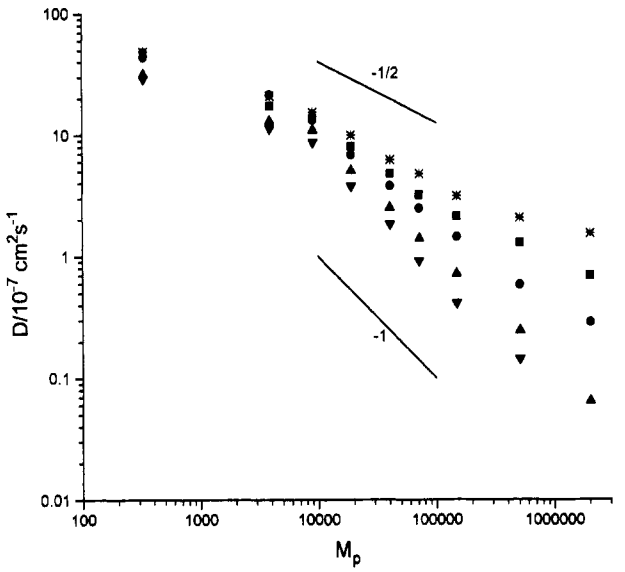

Figure 3. Diffusion coefficient as a function of probe molecular weight at various weight fractions of HPC: 0 (*); 0.004 53 (■); 0.010 70 (●); 0.024 22 (▲); 0.038 71 (▼). Slopes of $-1/2$ and -1 are indicated for reference.

pure water, $D_s \sim M_p^{-0.44\pm0.03}$ when evaluated over the entire range of molecular weights. Ignoring the two highest molecular weights gives instead an exponent of −0.53 ± 0.02. These values bracket the results of previous hydrodynamic measurements[44-46] in water, which are nicely summarized by Smit et al.[40] The value −0.53 for the shorter fragments appears to be the most negative exponent ever observed for dextrans; it is consistent with a linear or randomly branched chain in a fairly good solvent. Given the large sensitivity to which molecular weights are used,

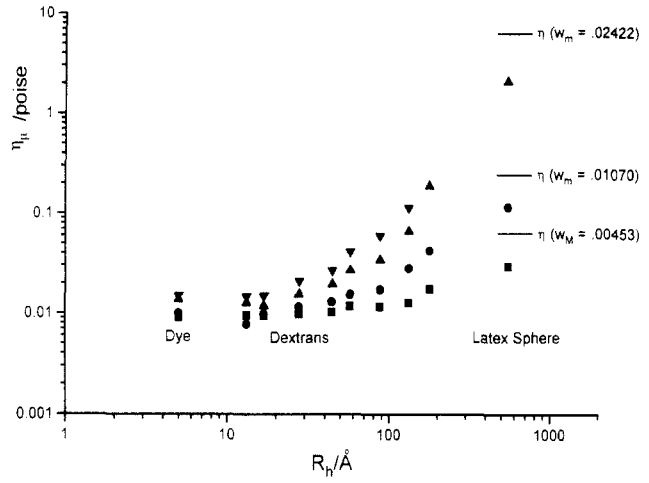

Figure 4. Microviscosities. Symbols are the same as in Figure 3. Horizontal lines show the macroscopic, zero-shear viscosity for comparison, except for the highest HPC concentration (omitted to provide a convenient scale for the rest and because the latex and FD-2000 probes were not measured for this HPC concentration; see Table 1).

and the polydispersity of the samples, there is little else to say about the M_p dependence of D_s in pure water.

A more important consideration is the change caused by increased HPC concentration. At the highest concentration of HPC-300 000 used, 3.871%, D_s becomes approximately dependent on M_p^{-1}, suggesting that screening of the hydrodynamic interactions has resulted in Rouse-type behavior. This interpretation requires some caution because HPC could have simultaneously induced contraction of the dextran chains. Contraction of a dilute linear random flight probe polymer in the presence of a second similar matrix polymer present at concentrations exceeding its overlap condition has been observed[47] to follow the predicted[48] scaling relationship $R_{g,probe} \sim c_{matrix}^{-1/8}$. We are not aware of similar predictions for mixtures of branched and semiflexible polymers but expect a similarly small effect. A simple argument can be made that the exponent describing the contraction of a coil in the presence of semiflexible rods should be $<1/8$.[49] Therefore, the simplest interpretation of the available data is that hydrodynamic screening is reached by $w_{HPC} \sim 0.04$. It is not clear whether the reptation exponent of −2, or an even higher exponent, would be observed at greater HPC concentrations.

Stokes–Einstein Relationship. Diffusion of a large particle of hydrodynamic radius R_h in a simple fluid of viscosity η_0 at temperature T is governed by the Stokes–Einstein relation, $D_s = k_B T/(6\pi\eta_0 R_h)$, where k_B is Boltzmann's constant. The relationship is not expected to hold for small diffusers in a complex, polymer-containing solution. A convenient way to gauge deviations from the Stokes–Einstein limit is via the microviscosity, $\eta_\mu = k_B T/(6\pi R_h D_s) \equiv f_s/(6\pi R_h)$, where f_s is the friction factor associated with self-diffusion. The increase of η_μ with probe size is shown for four concentrations of HPC-300 000 in Figure 4. The values of R_h in water were used to compute η_μ—i.e., possible contraction of the dextran probes was ignored. Failures of the Stokes–Einstein relationship are significant for all probes—even the largest latex probe, which is not subject to contraction. Larger probes (limited aggregates of latex particles with $R_h \sim$ 1000–2000 Å) were observed previously by dynamic light scattering to obey the Stokes–Einstein relationship more closely in HPC of similar molecular weight[9] although significant deviations did occur for spheres of radius R = 907 Å in HPC-1 000 000.[10] The magnitude by which latex probes in HPC fail to obey the Stokes–Einstein relationship is the subject of debate. All previous studies[5-10,50] have used dynamic light scattering, and the well-documented nonexponential character of autocorrelation functions from ternary solutions must be taken into consideration. Some of the disagreement undoubtedly traces to differences in just how this is accomplished.[10,50] For example, at moderate concentrations, latex spheres in HPC exhibit a surprisingly fast decay mode. Causes for this have been considered;[10] one possibility is that the fast decay mode represents cooperative motions of the polymer matrix. For an entry into the literature surrounding this phenomenon, see refs 18 and 28. Isolating the dominant slow mode from the fast mode (which becomes increasingly prominent as matrix concentration is increased) reduces the difference between the measured D (from the slow mode) and the Stokes–Einstein expectation.[10,50] Associating the initial decay rate of the autocorrelation function with the diffusion coefficient of the latex has the opposite effect. Thus, interpretation of dynamic light scattering data from ternary systems in terms of meaningful diffusion coefficients is nontrivial. A recent dynamic light scattering study by Phillies, Richardson, Quinlan, and Ren[50] reports large (i.e., factors of ≈100) failures for a latex probe with R = 335 Å in aqueous HPC. The failures, like the nonexponentiality, increased with HPC matrix concentration and seemed to indicate excessively rapid motion of the latex particles. This is counterintuitive, since the correlation length decreases with added polymer, making the matrix seem more like a continuum to the probe (see below). In a 2.5% solution of HPC-300 000 the 335-Å latex of ref 50 appears to diffuse about 20 times faster than Stokes–Einstein would predict. The latex probe in the present study is bigger, R = 551 Å, but the slightly larger size alone probably cannot account for the much closer adherence to Stokes–Einstein behavior demonstrated in Figure 4 (the failure is by a factor 2–3, and is not strongly dependent on concentration in our measured range). In comparing light scattering and FPR results, one must also consider not only the complete absence of modes related to the unlabeled polymer matrix in the latter technique but also the very different distance scales probed by the two methods. The distance scale of quasielectric light scattering is usually small, even if experiments are conducted at multiple scattering vectors. For example, a scattering angle of θ = 90° at incident wavelength λ_0 = 6328 Å corresponds to a distance scale of $2\pi/q$ = 3400 Å, where q is the scattering vector $(4\pi n \sin(\theta/2)/\lambda_0$ where n = solution refractive index). Thus, under the conditions of measurement employed in ref 50 the latex is observed to diffuse a distance only 5 times its own diameter. This is certainly adequate for a latex particle in a simple binary solution, but perhaps the long-term behavior will not be reached over such small distance scales in an entangled polymer mixture. At θ = 30° the distance scale $2\pi/q$ rises, but only to about 1 μm. The distance scale of FPR measurements, $2\pi/K$, is typically 1 or 2 orders of magnitude larger yet. This means that short-time motions cannot be observed; on the positive side, the long-term behavior is unambiguously measured. It is not clear whether the nonexponential character of the correlation functions, distance scale effects, or other factors are responsible for the very large failures of the Stokes–Einstein relation observed in some dynamic light scattering investigations of latex spheres in HPC-300 000.

Other Analyses. Langevin and Rondelez[51] proposed a simple stretched exponential to describe the enhanced

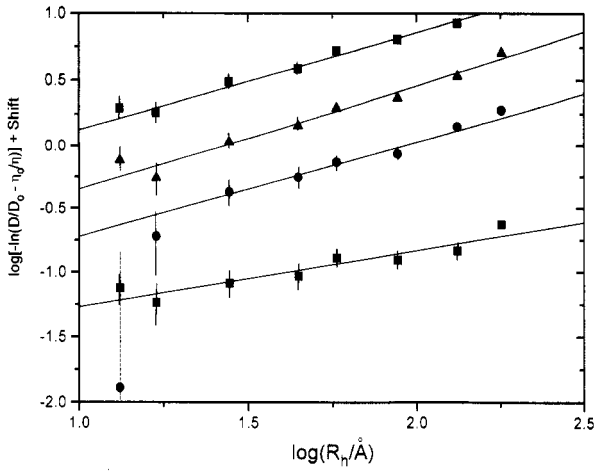

Figure 5. Langevin–Rondelez plot for dextran probes. See text and eq 1. Symbols are the same as in Figure 3. The largest dextran was not measured at the highest HPC concentration. For clarity, the curves are shifted arbitrarily along the ordinate. Error bars are computed for ±10% uncertainty in $D/D_0 - \eta_0/\eta$. The dashed error bar in the lower left corner overlaps two data points but belongs to the solid circle. It extends downward to $-\infty$.

diffusion of small probes in complex media:

$$D_s/D_0 = \eta_0/\eta + \exp[-(R_h/\xi)^\delta] \quad (1)$$

Here, D_0 and η_0 are the diffusion coefficient of the probe in pure solvent and the viscosity of the pure solvent, respectively. The continuum result expected for hard spheres is recovered when the probe size greatly exceeds the correlation length, ξ. The equation is intended for semidilute solutions ($\xi \ll R_g$, where R_g is the radius of gyration of the matrix polymer). The parameter δ is expected to be 2.5 for rigid gel matrices where the viscosity ratio on the right-hand side of eq 1 drops out; in solutions δ should be less. Equation 1 has the linearized form $\log(-\ln(D_s/D_0 - \eta_0/\eta)) = \delta \log R_h - \delta \log \xi$ from which both δ and ξ may be obtained. Figure 5 shows the appropriate plots for dextran probes at the four concentrations of HPC studied. The error bars were computed uniformly at ±10% for the quantity $D_s/D_0 - \eta_0/\eta$ in order to demonstrate the effect of the double-logarithmic data compression. The function $y = \log(-\ln(z))$ diverges at $z = 0$ and $z = 1$ corresponding respectively to the success and failure of the Stokes–Einstein relation when $z = D_s/D_0 - \eta_0/\eta$. Experimental errors at either of these limits are magnified, and the effects can be dramatic for the smaller probes. Nevertheless, linear behavior is observed throughout much of the probe size range. Parameters ξ and δ from unweighted linear fits to the linear regime appear in Table 1, where the subscript "LR" refers to ξ and δ values determined from eq 1. A very large uncertainty is associated with ξ_{LR} when it is extracted from the linearized equation. Therefore, Table 1 also shows the results of unweighted nonlinear least-squares fits to $D_s/D_0 - \eta_0/\eta$ vs R_h, which were performed using Origin Version 2.67 (MicroCal, Amherst, MA); several initial guesses were tried, leading to the same final results. There appears to be no particular trend to δ_{LR}. The average value is 0.63—not very different from the result, $\delta = 0.59$, found by Park et al.[52] for diffusion of mesoscopic probes in a permanent network. The cube root of the molecular volume, $\xi_v = (M_m/c_m N)^{-1/3}$ where N is Avogadro's number, always exceeds ξ_{LR}. The Langevin–Rondelez correlation length drops rapidly with matrix concentration, $\xi_{LR} \sim c_m^{-x}$ with $x = 0.87 \pm 0.03$; see Figure 6. The expected exponent for a random coil in a good solvent is $x = {}^3/_4$;[48] for a rod, one expects $x = {}^1/_2$ theoretically[53,54] and perhaps a little less

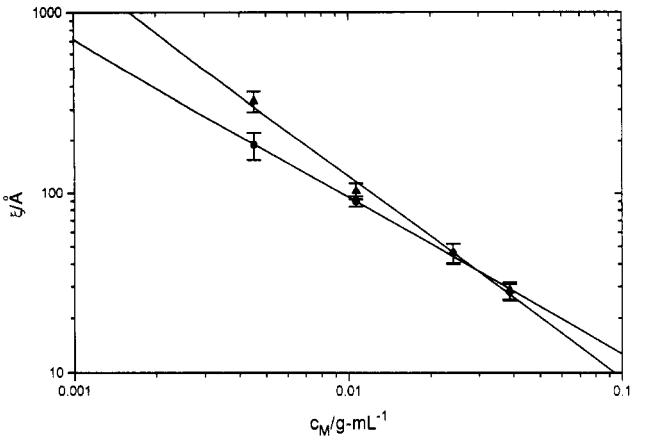

Figure 6. Correlation lengths determined from eq 1 (●) and eq 2b (▲).

experimentally.[55] The high exponent observed for HPC, which has intermediate flexibility, is surprising.

A somewhat more general expression is often used, in which the explicit viscosity dependence appropriate for solid spherical diffusers is subsumed into generalized matrix concentration and probe size dependencies:

$$D_s/D_0 = \exp(-\alpha c^\nu) \quad \text{at constant } R_h \quad (2a)$$

$$D_s/D_0 = \exp[-(R/\xi)^\delta] \quad \text{at constant } c \quad (2b)$$

The theories of Cukier,[56] Altenberger and Tirrell,[57] and Ogston and co-workers[58,59] all argue that $\nu = 0.5$. In the hydrodynamic scaling model proposed by Phillies[3,60] ν is predicted to vary from 0.5 for large M_p to 1 for small M_p; these values bracket most of the experimental results. The parameters α and ν obtained from an unweighted nonlinear least-squares analysis according to eq 2a appear in Table 1. Correlation lengths similarly obtained from eq 2b are shown in Table 1 and Figure 6 as ξ_{HS}; they differ from those estimated via eq 1 at low c_m, but again the concentration dependence is very strong. There is no particular trend in ν, except that it tends to be somewhat less than unity (when it can be reliably estimated at all). The present study is designed primarily to test the effect of probe size and spans a limited concentration range with only a few points, so we do not consider the ν values here to be definitive; however, similar ν values were observed in a study of the concentration effect in dextran/dextran/water.[15] The considerable variation of α with probe molecular mass is certainly significant. The hydrodynamic scaling model predicts (eq 41 of ref 3) that the concentration prefactor $\alpha \sim (M_p/M_m)^{1/2}$. Figure 7 shows that this is plausible, at least insofar as the M_p dependence is concerned.

Johansson, Elvingson, and Lofroth[61] have developed a theory based on Ogston's model for diffusion in a network of fibers.[58,59] The probe is assumed to be a compact sphere. This theory predicts D_s/D_0 given the fiber cross-sectional radius, a, and probe radius, R. The result is

$$D_s/D_0 = e^{-\kappa} + \kappa^2 e^\kappa E_1(2\kappa) \quad (3)$$

where $\kappa = \phi(R + a)^2/a^2$, ϕ is the matrix volume fraction, and $E_1(x) = \int_x^\infty e^{-u}/u\, du$. Accurate polynomial expressions for $E_1(x)$ are given in ref 62. Equation 3 fits our previously published data[11] for the sodium salt of fluorescein dye in HPC at various molecular weights if it assumed that a = 3 Å.[63] Figure 8 compares eq 3 to the dextran diffusion data measured in a 1.070% HPC-300 000 solution, assuming a = 5, 10, and 20 Å and also assuming $R = R_h$. Results at other HPC concentrations were qualitatively

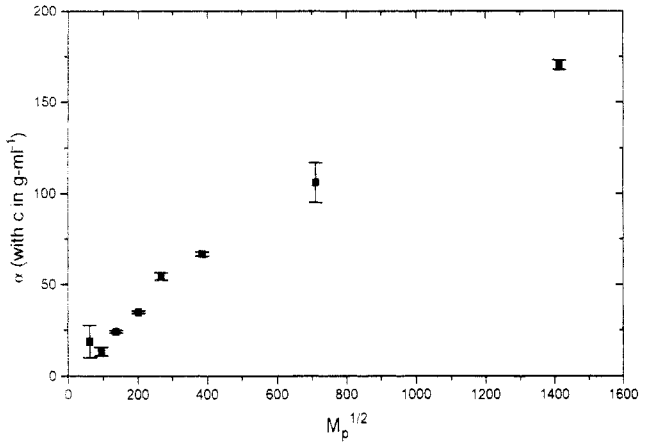

Figure 7. Parameter α from eq 2a increases with probe molecular weight.

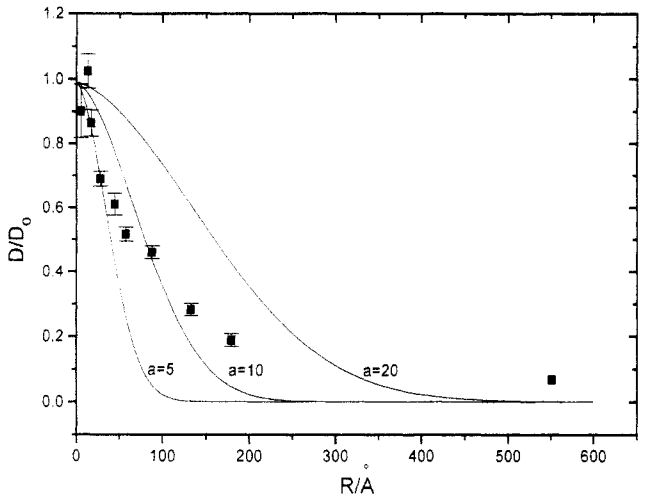

Figure 8. Reduction of diffusion with probe radius for w_{HPC} = 0.010 70. Curves represent the behavior of the Johansson–Elvingson–Lofroth model (eq 3) for assumed matrix radii of 5, 10, and 20 Å, as indicated.

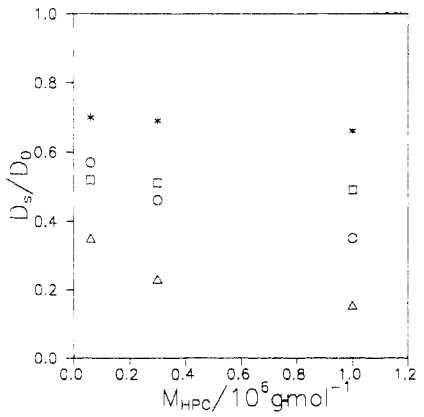

Figure 9. Small probes care little what the matrix molecular weight is, while large probes are sensitive to matrix molecular weight: (*) FD-20 in 1.069% HPC; (○) FD-150 in 1.069% HPC; (□) FD-20 in 2.422% HPC; (△) FD-150 in 2.422% HPC.

similar—that is, eq 3 comes close at low R if a = 5 Å is assumed but underestimates diffusion at larger R. The probes in the present study are larger and/or more complex structurally than those shown previously[61] to agree with eq 3. However, it is not possible to identify a specific mechanism, such as reptation, that might account for the rapid diffusion at high concentrations.

Effect of Matrix Molecular Weight. Figure 9 shows that small dextran probes are relatively insensitive to matrix molecular weight, similar to free dye.[11] This is sensible, because matrix polymers of any molecular weight are virtually at a standstill compared to a small dye, and the reduction of diffusion is largely a function of the space occupied by the matrix. Larger probes are more highly sensitized to the macroscopic viscosity, which depends strongly on molecular weight for the semiflexible HPC.

Probe Structural Effects. Differences between the spherical latex probe and dextran chains are difficult to discern from the present data. Such differences are expected[23,24] for a linear chain probe that has crossed over to the reptation regime, thereby gaining a diffusion mechanism not available to the hard sphere. This assumes that reptation occurs in solution, which remains controversial.[3,16,64] Differences between similarly sized linear and spherical probes have been seen elsewhere under conditions thought to favor reptation.[64] However, the linear chains diffused more slowly, not more rapidly, than the spheres. As the reptation molecular weight exponent of −2 was not observed in Figure 3, it is not surprising that dramatic differences between spheres and chains were not observed in the present study.

Nonexponential FPR Profiles: Analytical Possibilities

Within the noise of the experiment, all the dextran standards appeared to give single-exponential FPR signals in water and dilute HPC solutions. The recovery profiles deviated slightly from a single-exponential form as c_m increased. The significant result of Figure 3 is that D becomes more strongly dependent on M_p as c_m is increased; thus, the decay rate distribution of a polydisperse sample becomes spread out. The deleterious consequences of this effect for probe diffusion experiments have been considered;[65] we do not believe the foregoing results are seriously affected, since the polydispersities are fairly small and since the D vs M dependence was never extreme at the HPC concentrations studied. Expansion of the D vs M dependence does, however, present new analytical opportunities. What follows is a small beginning to explore the feasibility of polymer characterization by FPR in systems containing a polymeric matrix.

It is appropriate to review the related dynamic light scattering experiment, as applied to polymer size or molecular weight distributions. Inverse Laplace transform (ILT) analysis of dynamic light scattering correlation functions has reached a fairly advanced state of development. The electric field autocorrelation function can generally be represented as a weighted sum of decaying functions:

$$g(\tau) = A_1 \exp(-\Gamma_1\tau) + A_2 \exp(-\Gamma_2\tau) + \ldots$$

The amplitude A_i is related to the concentration, size, and molecular weight of the species i, while the decay rate Γ_i depends on the diffusion coefficient D_i and the spatial frequency of the light scattering experiment (i.e., $\Gamma_i = q^2D_i$, where q is the scattering vector). After establishing relationships between D and M using standards, it is possible to determine concentration vs M distributions. The method has many useful applications (high-temperature systems, caustic solvents, samples with a very wide molecular weight distribution, etc.). Its biggest limitation is poor resolution; it is generally not possible to resolve components unless their associated decay rates differ by a factor exceeding about 2 and then only when the associated amplitudes of both are significant. A tough case occurs for random-flight polymers (say, $D \sim M^{-0.5}$) containing small quantities by weight of a low-mass component. Analysis of such polymers is commonly

conducted in the presence of a matrix—typically by gel permeation chromatography or, for charged polymers, by gel electrophoresis. In their most common configurations, both techniques require calibration. Dynamic light scattering in a polymer matrix and coupled to ILT analysis could compete with these techniques, in principle, but the scattering from the matrix would have to be almost completely extinguished by careful index matching, the required samples are large compared to FPR, and their cleanliness is of utmost importance. The polymer must be compatible with the matrix and yet must be present at a concentration sufficient to give a strong scattering signal. Then, the experiment should be repeated to ensure that the concentration is sufficiently low. Finally, there is nothing one can do to prevent large polymers from greatly outscattering small ones, even when the latter are numerically more prevalent. Little wonder that the effects of polydispersity on dynamic light scattering from ternary systems have been considered primarily as a nuisance to fundamental mobility studies, instead of a polymer characterization opportunity.

In an FPR experiment with modulation detection, each diffusing component contributes a single exponential to the ac recovery:

$$\mathrm{ac}(t) = A_1 \exp(-\Gamma_1 t) + A_2 \exp(-\Gamma_2 t) + \ldots$$

Let us assume that the fluorescent intensity of a single fluorophore does not depend on the molecular weight of the macromolecule to which it is attached. We also assume independence of photobleachability and chemical recovery effects on polymer molecular weight. Then the amplitudes A_i are given by $A_i \sim n_i F_i$, where n_i is the number density of species i and F_i the number of fluorophores attached to that species. Two cases are of special importance: singly labeled polymers and polymers where the number of labels is proportional to the molecular weight. The former case, $F_i = 1$ for all i, represents typical end-labeling schemes (e.g., termination of addition polymerization with a fluorescent dye). The proportional case would ordinarily pertain to most side-chain substitution labeling schemes or copolymerization with a fluorescent comonomer. For proportionally labeled polymers, let $F_i = p\sigma_i$, where p is the probability of a monomer selected at random being labeled, assumed to be independent of i, and σ_i is the degree of polymerization of species i. This is analogous to weighting by mass and should produce a weight-average diffusion coefficient from the initial, or average, recovery rate. The singly labeled case corresponds to number weighting and leads to a number-average diffusion coefficient; this mode of labeling keeps the small diffusers from being overwhelmed by the larger ones. Dynamic light scattering produces a z-average diffusion coefficient[66] since the intensity scattered by a polymer is proportional to $n_i M_i^2$. Either fluorescent labeling scheme can take advantage of a wide range of matrices, including especially those made from a sample of the identical polymer without fluorescent label to prevent compatibility problems. Thanks to the high sensitivity of FPR, concentrations can be kept very low, so that extrapolation to zero probe concentration would ordinarily be unnecessary. These features combine with a very small sample size (several microliters) and trivial sample preparation, impervious to "dust", to make analysis by FPR appealing. The obvious disadvantage of the technique is the need to attach an appropriate dye; however, compared to the immutable limitations of some methods (e.g., gel electrophoresis, which requires permanent charge) even this seems tolerable.

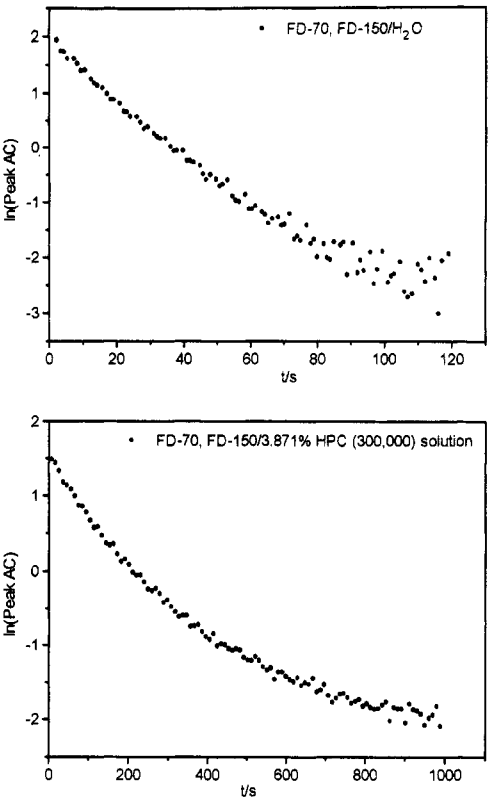

Figure 10. Semilogarithmic plot of a binary mixture of dextrans FD-70 and FD-150 in water (straighter, top curve) and 3.871% HPC. The dextran composition is such that the fluorescent intensity arising from each dextran fraction is approximately the same.

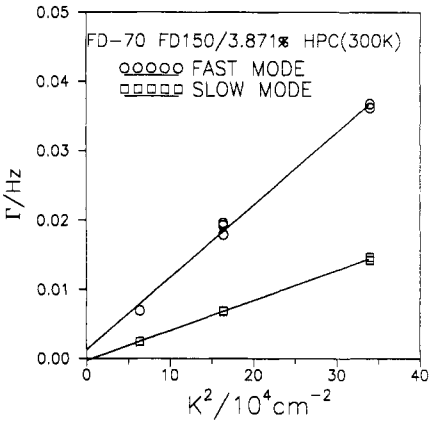

Figure 11. The fast and slow modes arising from the two dextran fractions are both diffusive, scaling with K^2.

In order to demonstrate the potential of the method, mixed dextrans were prepared. Binary solutions were adjusted to give similar fluorescence intensities and then mixed evenly in water and an HPC matrix solution. The recovery signal in water scarcely deviated from a single exponential, within the noise of the experiment. The recovery signal in 3.871% HPC, shown in Figure 10, clearly deviates from a single-exponential form, even though the two dextrans differ in hydrodynamic size by a factor of only 1.5. Figure 11 shows that both the slow and fast decay rates for the same sample vary as K^2—i.e., they are diffusive. From the slopes, we can evaluate the diffusion coefficients of the two mixed species. These diffusion coefficients could be compared to a calibration plot (similar to Figure 1, but with R_h as the abscissa) to obtain the size of the two probes. For the purpose of demonstrating the feasibility of the method, it is adequate to determine just the diffusion coefficients. Table 2 compares D values

Table 2. Ability of FPR to Resolve Mixed Dextran Fractions in an HPC Matrix

	$D/10^{-8}$ cm^2 s^{-1}		
	measd alone in HPC	measd as a binary mixture in HPC	error/%
	In 3.871% HPC (300 K) Solution		
FD-70	9.19	10.4	12
FD-150	4.15	4.34	5
	In 2.861% HPC (300 K) Solution		
FD-70	11.60	13.25	14
FD-150	5.52	4.34	21
FD-40	22.07	22.56	2
FD-150	5.52	4.58	17

determined from mixtures of dextrans resolved in an HPC matrix with the values obtained from each component measured separately in the same HPC matrix. Accuracy improves with increased HPC concentration or increased separation in size. Much remains to be done to develop analytical applications of FPR. However, its many benefits and the present preliminary results suggest that the effort may be worthwhile. The one-shot FPR experiment is inherently noisy compared to dynamic light scattering, where long acquisitions can produce data of vanishingly small noise content (for perfectly clean samples anyway). Efforts to reduce the noise in FPR signals are underway.

Acknowledgment. This work was supported by NSF award DMR-8914604 and the Louisiana Stimulus for Excellence in Research, with some equipment being provided by the Lousiana Educational Quality Support Fund. The creative contributions of Mr. George Gascon and Mr. Don Patterson to the construction of the FPR device are gratefully acknowledged.

References and Notes

(1) Turner, D. N.; Hallett, F. R. *Biochem. Biophys. Acta* **1976**, *451*, 305.
(2) Lin, T.-H.; Phillies, G. D. J. *Macromolecules* **1984**, *17*, 1686.
(3) Phillies, G. D. J. *J. Phys. Chem.* **1989**, *93*, 5029.
(4) Ullmann, G. S.; Ullmann, K.; Lindner, R. M.; Phillies, G. D. J. *J. Phys. Chem.* **1985**, *89*, 692.
(5) Phillies, G. D. J.; Clomenil, D. *Macromolecules* **1993**, *26*, 167.
(6) Jamieson, A.; Southwick, J.; Blackwell, J. *J. Polym. Sci., Polym. Phys. Ed.* **1982**, *20*, 1513.
(7) Rymden, R.; Brown, W. *Macromolecules* **1986**, *19*, 2942.
(8) Yang, T.; Jamieson, A. M. *J. Colloid Interface Sci.* **1988**, *126*, 220.
(9) Russo, P. S.; Stephens, L. K.; Cao, T.; Mustafa, M. *J. Colloid Interface Sci.* **1988**, *122*, 120.
(10) Mustafa, M.; Russo, P. S. *J. Colloid Interface Sci.* **1989**, *129*, 240.
(11) Mustafa, M. B.; Tipton, D. L.; Barkley, M. D.; Russo, P. S.; Blum, F. D.; *Macromolecules* **1993**, *26*, 370.
(12) Tracy, M.; Pecora, R. *Macromolecules* **1992**, *25*, 337.
(13) Brown, W.; Rymden, R. *Macromolecules* **1988**, *21*, 840.
(14) Onyenemezu, C. N.; Gold, D.; Roman, M.; Miller, W. G. *Macromolecules* **1993**, *26*, 3833.
(15) Furukawa, R.; Arauz-Lara, J. L.; Ware, B. R. *Macromolecules* **1991**, *24*, 599.
(16) Lodge, T. P.; Rotstein, N. A.; Prager, S. *Adv. Chem. Phys.* **1990**, *LXXIX*, 1.
(17) Borsali, R.; Duval, M.; Benoit, H.; Benmouna, M. *Macromolecules* **1987**, *20*, 1112.
(18) Borsali, R.; Duval, M.; Benmouna, M. *Macromolecules* **1989**, *22*, 816.
(19) Kent, M. S.; Tirrell, M.; Lodge, T. P. *Macromolecules* **1992**, *25*, 5383.
(20) Lodge, T. P. *Macromolecules* **1983**, *16*, 1393.
(21) Chang, T.; Han, C. C.; Wheeler, L. M.; Lodge, T. P. *Macromolecules* **1988**, *21*, 1870.
(22) Lodge, T. P.; Wheeler, L. M. *Macromolecules* **1986**, *19*, 2983.
(23) Martin, J. E. *Macromolecules* **1986**, *19*, 922.
(24) Martin, J. E. *Macromolecules* **1984**, *17*, 1279.
(25) Chu, B.; Wu, D.-Q. *Macromolecules* **1987**, *20*, 1606.
(26) Lodge, T. P.; Markland, P.; Wheeler, L. M. *Macromolecules* **1989**, *22*, 3409.
(27) Wheeler, L. M.; Lodge, T. P. *Macromolecules* **1989**, *22*, 3399.
(28) Akcasu, A. Z.; Nagele, G.; Klein, R. *Macromolecules* **1991**, *24*, 4408.
(29) Hervet, H.; Leger, L.; Rondelez, F. *Phys. Rev. Lett.* **1979**, *42*, 1681.
(30) Ware, B. R. *Am. Lab.* **1984**, *16*, 16.
(31) Lanni, F.; Ware, B. R. *Rev. Sci. Instrum.* **1982**, *53* (6), 905.
(32) Swensen, H. A.; Schmitt, C. A.; Thomson, N. S. *J. Polym. Sci., Part C* **1965**, *11*, 243.
(33) Kamide, K.; Saito, M.; Suzuki, H. *Makromol. Chem., Rapid Commun.* **1983**, *4*, 33.
(34) Aharoni, S. M. *Macromolecules* **1983**, *16*, 1722.
(35) Werbowyj, R. S.; Gray, D. G. *Mol. Cryst. Liq. Cryst. Lett.* **1976**, *34*, 97.
(36) Werbowyj, R. S.; Gray, D. G. *Macromolecules* **1980**, *13*, 69.
(37) Robitaille, N.; Turcotte, N.; Fortin, S.; Charlet, G. *Macromolecules* **1991**, *24*, 2413.
(38) Burton, B. A.; Brant, D. A. *Biopolymers* **1983**, *22*, 1769.
(39) Garg, S. K.; Stivala, S. S. *J. Polym. Sci., Polym. Phys. Ed.* **1978**, *16*, 1419.
(40) Smit, J. A. M.; van Dijk, J. A. P. P.; Mennen, M. G.; Daoud, M. *Macromolecules* **1992**, *25*, 3585.
(41) Chang, T.; Yu, H. *Macromolecules* **1984**, *17*, 115.
(42) Mustafa, M. B.; Tipton, D.; Russo, P. S. *Macromolecules* **1989**, *22*, 1500.
(43) Horowitz, P.; Hill, W. *The Art of Electronics*; Cambridge University Press: Cambridge, U.K., 1980; p 118.
(44) Senti, F. R.; Hellman, N. N.; Ludwig, N. H.; Babcock, G. E.; Tobin, R.; Glass, C. A.; Lamberts, B. L. *J. Polym. Sci.* **1955**, *17*, 527.
(45) Snabre, P.; Grossmann, G. H.; Mills, P. *Colloid Polym. Sci.* **1985**, *263*, 478.
(46) Sellen, D. B. *Polymer* **1975**, *16*, 561.
(47) Kent, M. S.; Tirrell, M.; Lodge, T. P. *Polymer* **1991**, *32* (2), 314.
(48) de Gennes, P.-G. *Scaling Concepts in Polymer Physics*; Cornell University Press: Ithaca, NY, 1979.
(49) Jamil, T.; Russo, P.; Negulescu, I.; Daly, W.; Schaefer, D. W.; Beaucage, G. *Macromolecules*, in press.
(50) Phillies, G. D. J.; Richardson, C.; Quinlan, C. A.; Ren, S. Z. *Macromolecules* **1993**, *26*, 6849.
(51) Langevin, D.; Rondelez, F. *Polymer* **1978**, *19*, 875.
(52) Park, I. H.; Johnson, C. S., Jr.; Gabriel, D. A. *Macromolecules* **1990**, *23*, 1548.
(53) de Gennes, P.-G.; Pincus, P.; Velasco, R. M.; Brochard, F. *J. Phys. (Paris)* **1976**, *37*, 1461.
(54) Shimada, T.; Doi, M.; Okano, K. J. *J. Chem. Phys.* **1988**, *88*, 2815.
(55) DeLong, L. M.; Russo, P. S. *Macromolecules* **1991**, *24*, 6139.
(56) Cukier, R. I. *Macromolecules* **1984**, *17*, 252.
(57) Altenberger, A. R.; Tirrell, M. *J. Chem. Phys.* **1984**, *80*, 2208.
(58) Ogston, A. G.; Preston, B. N.; Wells, J. D.; Snowden, J. McK. *Proc. R. Soc. London Ser. A* **1973**, *333*, 297.
(59) Ogston, A. G. *Trans. Faraday Soc.* **1958**, *54*, 1754.
(60) Phillies, G. D. J. *Macromolecules* **1986**, *19*, 2367.
(61) Johansson, L.; Elvingson, C.; Lofroth, J. E. *Macromolecules* **1991**, *24*, 6024.
(62) Abramowitz, M.; Stegun, I. A. *Handbook of Mathematical Functions with Formulas, Graphs and Mathematical Tables*; National Bureau of Standards: Washington, DC, 1964.
(63) Lofroth, J. E., private communication.
(64) Phillies, G. D. J.; Brown, W.; Zhou, P. *Macromolecules* **1992**, *25*, 4948.
(65) Lodge, T. P.; Wheeler, L. M.; Hanley, B.; Tirrell, M. *Polym. Bull. (Berlin)* **1986**, *15*, 35.
(66) Koppel, D. E. *J. Chem. Phys.* **1972**, *57*, 4814.
(67) Mustafa, M. M. Ph.D. Thesis, Louisiana State University, Baton Rouge, LA, 1990.